AMERICAN SOCIETY of
GENE & CELL
THERAPY

MicroRNA-29a-3p Reduces TNFα-Induced Endothelial Dysfunction by Targeting Tumor Necrosis Factor Receptor 1

Xinrui Deng,[1,4] Xia Chu,[1,4] Peng Wang,[1] Xiaohui Ma,[1] Chunbo Wei,[1] Changhao Sun,[1,2] Jianjun Yang,[3] and Ying Li[1,2]

[1]Department of Nutrition and Food Hygiene, Public Health College, Harbin Medical University, No. 157 Baojian Road, Nangang District, Harbin 150081, China; [2]Research Institute of Food, Nutrition and Health, Sino-Russian Medical Research Center, Harbin Medical University, No. 157 Baojian Road, Nangang District, Harbin 150081, China; [3]Department of Nutrition and Food Hygiene, School of Public Health and Management, Ningxia Medical University, No. 1160 Shengli Road, Xingqing District, Yinchuan 750004, China

miR-29a-3p has been shown to be associated with cardiovascular diseases; however, the effect of miR-29a-3p on endothelial dysfunction is unclear. This study aimed to reveal the effects and mechanisms of miR-29a-3p on endothelial dysfunction. The levels of vascular cell adhesion molecule 1 (VCAM-1), intercellular adhesion molecule 1 (ICAM-1), and E-selectin were determined by real-time PCR and immunofluorescence staining to reveal the degree of tumor necrosis factor alpha (TNFα)-induced endothelial dysfunction. A luciferase activity assay and cell transfection with a miR-29a-3p mimic or an inhibitor were used to reveal the underlying mechanisms of miR-29a-3p action. Furthermore, the effects of miR-29a-3p on endothelial dysfunction were assessed in C57BL/6 mice injected with TNFα and/or a miR-29a-3p agomir. The results showed that the expression of TNFα-induced adhesion molecules in vascular endothelial cells (EA.hy926 cells, human aortic endothelial cells [HAECs], and primary human umbilical vein endothelial cells [pHUVECs]) and smooth muscle cells (human umbilical vein smooth muscle cells [HUVSMCs]) was significantly decreased following transfection with miR-29a-3p. This effect was reversed by cotransfection with a miR-29a-3p inhibitor. As a key target of miR-29a-3p, tumor necrosis factor receptor 1 mediated the effect of miR-29a-3p. Moreover, miR-29a-3p decreased the plasma levels of TNFα-induced VCAM-1 (32.62%), ICAM-1 (38.22%), and E-selectin (39.32%) *in vivo*. These data indicate that miR-29a-3p plays a protective role in TNFα-induced endothelial dysfunction, suggesting that miR-29a-3p is a novel target for the prevention and treatment of atherosclerosis.

INTRODUCTION

Atherosclerosis is a chronic multifactorial vascular disease that is considered to be the leading cause of morbidity and mortality among cardiovascular diseases worldwide.[1–3] There is growing evidence that endothelial dysfunction may be the cause of important early events in atherosclerosis that promote the development and progression of plaques.[4–7] Endothelial dysfunction is commonly detected by the elevation of soluble markers, such as adhesion molecules, including vascular cell adhesion molecule 1 (VCAM-1), intercellular adhesion molecule 1 (ICAM-1), and E-selectin.[8–11] However, the detailed mechanisms leading to endothelial dysfunction remain incompletely understood.

MicroRNAs (miRNAs, miRs) are short (21–23 nt) noncoding RNAs that regulate target genes by degrading mRNAs or by inhibiting posttranscriptional gene expression by binding to partially complementary mRNA recognition sequences.[12,13] miRNAs have been implicated in the control of a number of biological functions, including metabolism, differentiation, development, proliferation, apoptosis, and oncogenesis.[14] Recently, the role of miRNAs in the pathogenesis and physiological processes of cardiovascular diseases has been frequently investigated,[15–19] and some miRNAs, including miR-29, have attracted significant attention.[20–24]

Previous studies have reported that miR-29 can play pivotal roles in the regulation of fibrosis in a variety of organs, such as hepatic fibrosis,[25,26] cardiac fibrosis,[20] renal fibrosis,[27] and pulmonary fibrosis.[28,29] In recent years, researchers have been concerned about the role of miR-29 in cardiovascular diseases.[21,23,24,30,31] Sassi et al.[23] reported that miR-29 promotes pathological hypertrophy and overall cardiac insufficiency of cardiac myocytes rather than fibrotic heart disease. These studies imply that miR-29 may be involved in the progression of cardiovascular diseases, although different studies suggest that the role of miR-29 in cardiac function or atherosclerosis is debatable. However, the role of miR-29 in

vascular endothelial function and its underlying mechanisms have not been determined.

In this study, we investigated the effect of miR-29a-3p on tumor necrosis factor alpha (TNFα)-induced endothelial dysfunction and its underlying mechanisms *in vitro* and *in vivo*. Here, we report for the first time that miR-29a-3p can ameliorate TNFα-induced endothelial dysfunction by targeting tumor necrosis factor receptor 1 (TNF-R1), which means that miR-29a may be a potential novel target for the early prevention of atherosclerosis.

RESULTS

miR-29a-3p Modulates VCAM-1, ICAM-1, and E-selectin Expression in EA.hy926 Cells, HAECs, pHUVECs, and HUVSMCs

To analyze the potential effect of miR-29a-3p on endothelial dysfunction, we assessed the levels of adhesion molecules, including VCAM-1, ICAM-1 and E-selectin, in EA.hy926 cells, human aortic endothelial cells (HAECs), primary human umbilical vein endothelial cells (pHUVECs), and human umbilical vein smooth muscle cells (HUVSMCs). As expected, the transfection of an exogenous miR-29a-3p mimic and a miR-29a-3p inhibitor significantly increased and decreased intracellular miR-29a-3p expression, respectively, suggesting successful transfection (Figures S1A–S1H).

Compared with the normal group, in the TNFα group, VCAM-1, ICAM-1, and E-selectin mRNA levels dramatically increased, whereas the transfection of EA.hy926 cells with miR-29a-3p mimic noticeably prevented VCAM-1, ICAM-1, and E-selectin production. In addition, transfection with a miR-29a-3p inhibitor enhanced the increases in ICAM-1 mRNA levels that were induced by TNFα. To test whether the changes were influenced by miR-29a-3p, the cells were cotransfected with the miR-29a-3p mimic and its inhibitor, and the effect of miR-29a-3p in the TNFα model was significantly diminished (Figures 1A–1C). These results suggested that miR-29a-3p modulated TNFα-induced expression of VCAM-1, ICAM-1, and E-selectin in EA.hy926 cells.

Furthermore, we examined the effect of miR-29a-3p on VCAM-1, ICAM-1, and E-selectin protein expression using immunofluorescence staining. A similar trend was observed in the protein levels of VCAM-1, ICAM-1, and E-selectin in EA.hy926 cells that was similar to what was observed in the mRNA level. The upregulation of miR-29a-3p dramatically decreased TNFα-induced VCAM-1 protein expression, and the inhibition effect was partly reversed by co-application with the miR-29a-3p inhibitor, while transfection with the miR-29a-3p inhibitor alone partly enhanced the effect of TNFα on VCAM-1, ICAM-1, and E-selectin expression (Figure 1D). Furthermore, TNFα-induced ICAM-1 and E-selectin protein expression, which was visualized with R-phycoerythrin (PE), was also affected by miR-29a-3p, and that was similar to what was observed for VCAM-1 (Figures 1E and 1F).

To further determine whether miR-29a-3p modulates TNFα-induced expression of adhesion molecules in other endothelial cells, VCAM-1, ICAM-1, and E-selectin expression was examined at both the mRNA and protein levels in HAECs (Figure 2) and pHUVECs (Figure 3). VCAM-1, ICAM-1, and E-selectin expression was increased in the presence of TNFα, and treatment with the miR-29a-3p mimic reduced their levels in HAECs and pHUVECs. Cotransfection with the miR-29a-3p inhibitor partly restored the expression of VCAM-1, ICAM-1, and E-selectin. In addition, transfection with the miR-29a-3p inhibitor alone increased TNFα-induced mRNA levels of VCAM-1, ICAM-1, and E-selectin in HAECs and pHUVECs. The results suggest that miR-29a-3p ameliorates TNFα-induced VCAM-1, ICAM-1, and E-selectin expression in three kinds of endothelial cell lines (EA.hy926 cells, HAECs, and pHUVECs).

Next, the effects of miR-29a-3p on TNFα-induced expression of adhesion molecule (VCAM-1, ICAM-1, and E-selectin) were assessed in HUVSMCs. TNFα strikingly upregulated VCAM-1, ICAM-1, and E-selectin expression at both the mRNA and protein levels in HUVSMCs. In the presence of TNFα, treatment with the miR-29a-3p mimic dramatically inhibited the increase in VCAM-1, ICAM-1, and E-selectin expression that was mediated by TNFα; however, co-application with the miR-29a-3p inhibitor restored the ICAM-1 mRNA level. Compared with the TNFα group, the miR-29a-3p inhibitor increased VCAM-1 and E-selectin expression at the mRNA level (Figures 4A–4C). The accumulation of VCAM-1, ICAM-1, and E-selectin proteins, which was measured by immunofluorescence staining, dramatically decreased in the miR-29a-3p mimic group and increased in the miR-29a-3p inhibitor group compared with the TNFα group; however, cotreatment with the miR-29a-3p inhibitor partially abrogated the effect of the miR-29a-3p mimic (Figures 4D–4F).

miR-29a-3p Specifically Suppresses the Levels of TNF-R1 Protein Expression

A bioinformatics analysis was performed by an online algorithm, TargetScan 6.2, to predict the potential targets of miR-29a-3p. Considering that the important influence of TNF-R1 on endothelial dysfunction is induced by pro-atherosclerotic cytokines, such as TNFα, we designed our experiments to test the connection between miR-29a-3p and TNF-R1. TargetScan predicted that the binding sequence in the 3′ UTR of *TNFRSF1A*, which encodes TNF-R1, was a very good match for the miR-29a-3p seed (Figure 5A). In addition, a luciferase assay revealed that miR-29a-3p overexpression inhibited luciferase activity in HEK293 cells transfected with a reporter plasmid carrying the wild-type (WT) 3′ UTR of *TNFRSF1A*; the luciferase activity of the mutated (Mut) TNF-R1 3′ UTR vector was unaffected by simultaneous transfection with the miR-29a-3p mimic (Figure 5B). Furthermore, the luciferase activity of the TNF-R1 3′ UTR WT or Mut was uninfluenced by miR-29a-3p inhibitor (Figure 5B).

To further confirm our luciferase results, similar transfection procedures were conducted in EA.hy926 cells, HAECs, pHUVECs, and HUVSMCs. The overexpression of miR-29a-3p decreased the TNF-R1 protein levels compared to those in the NC group, and cotreatment with the miR-29a-3p inhibitor partly attenuated the miR-29a-3p-mediated downregulation of TNF-R1 expression, while
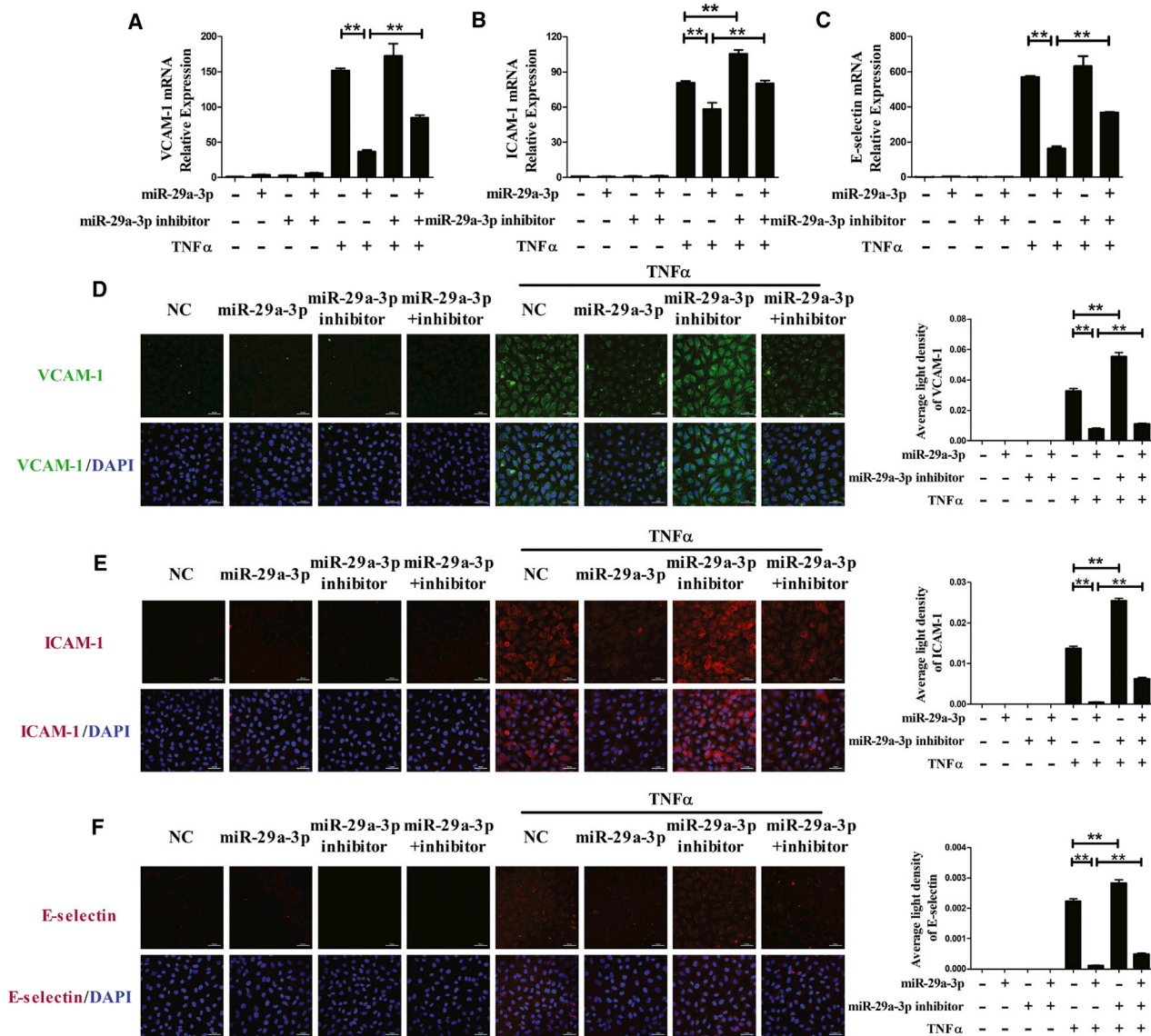
Figure 1. miR-29a-3p Modulates TNFα-Induced VCAM-1, ICAM-1 and E-selectin Expression in EA.hy926 Cells

(A–F) The mRNA levels of VCAM-1 (A), ICAM-1 (B), and E-selectin (C) were detected, and the protein expression levels of VCAM-1 (D), ICAM-1 (E), and E-selectin (F) were analyzed by immunofluorescence staining in differentially transfected EA.hy926 cells. The nuclei were counterstained with DAPI (blue). Each experiment was performed at least three times. EA.hy926 cells were transfected with miR-29a-3p or/and miR-29a-3p inhibitor for 48 h and then treated with or without TNFα for 3 h (mRNA detection) or for 6 h (protein detection). A scrambled sequence was used as a negative control (NC). Error bars are defined as the SD. Scale bars, 50 μm. *p < 0.05 and **p < 0.01 indicate statistically significant differences. miR-29a-3p, cells transfected with miR-29a-3p mimic; miR-29a-3p inhibitor, cells transfected with miR-29a-3p inhibitor; miR-29a-3p-+inhibitor, cells transfected with miR-29a-3p mimic and its inhibitor.

treatment with the miR-29a-3p inhibitor alone increased the protein levels of TNF-R1 (Figures 5C–5F). Collectively, the above data suggest that TNF-R1 is a genuine target of miR-29a-3p.

miR-29a-3p Affect TNFα-Induced VCAM-1, ICAM-1, and E-selectin Expression by Targeting TNF-R1

In summary, the miR-29a-3p mimic specifically suppressed TNF-R1 expression and modulated TNFα-induced VCAM-1, ICAM-1, and

E-selectin expression. To further verify that miR-29a-3p affects TNFα-induced VCAM-1, ICAM-1, and E-selectin expression by targeting TNF-R1, pHUVECs were cotransfected with the miR-29a-3p mimic and a TNF-R1-overexpression plasmid, or they were cotransfected with the miR-29a-3p inhibitor and a TNF-R1-small interfering RNA (siRNA). Transfection with the TNF-R1-overexpression plasmid or the TNF-R1-siRNA significantly increased or decreased intracellular TNF-R1 protein expression,
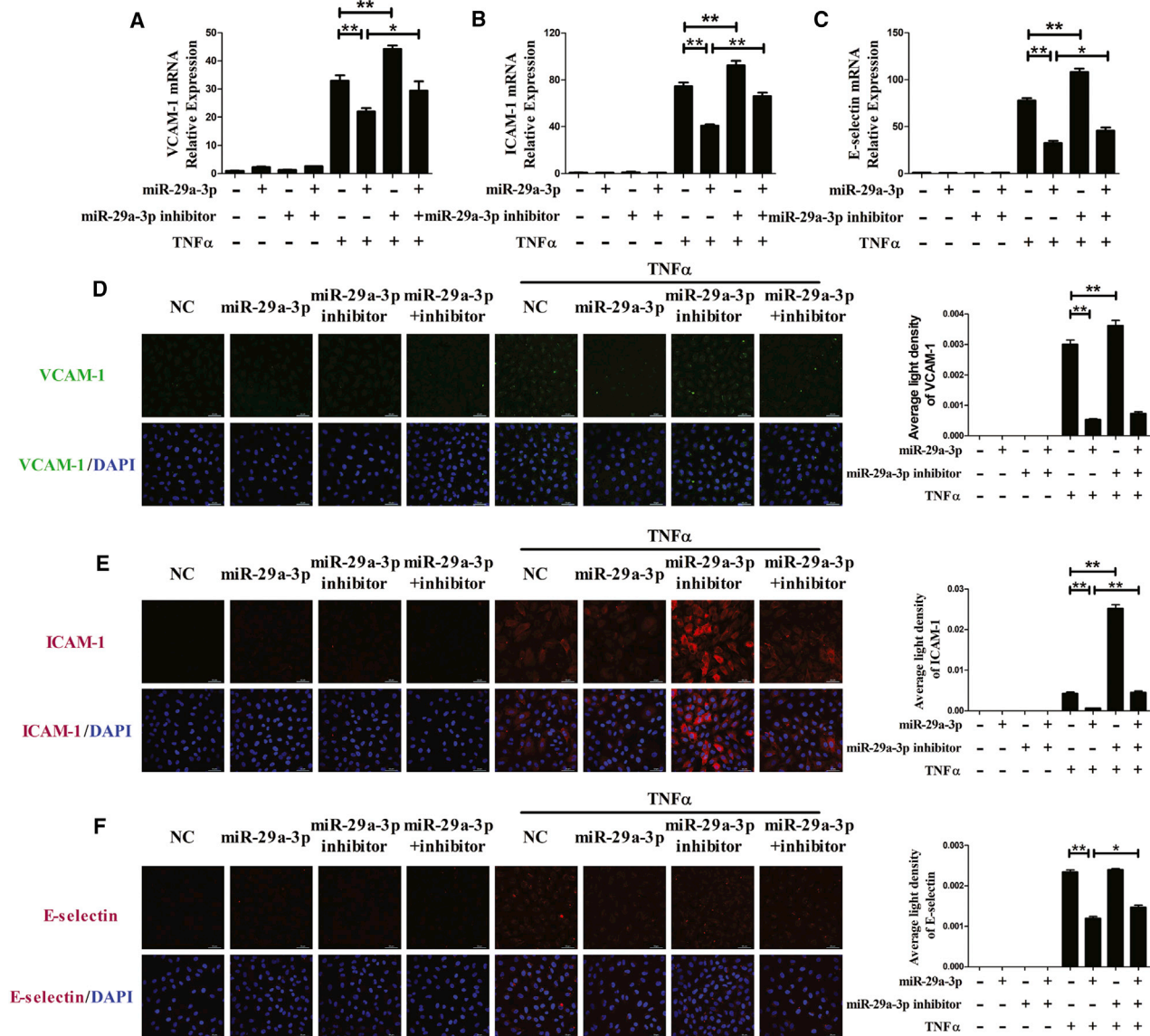
Figure 2. miR-29a-3p Modulates TNFα-Induced VCAM-1, ICAM-1, and E-selectin Expression in HAECs

(A–F) The mRNA levels of VCAM-1 (A), ICAM-1 (B), and E-selectin (C) were detected, and the protein expression levels of VCAM-1 (D), ICAM-1 (E), and E-selectin (F) were analyzed by immunofluorescence staining in differentially transfected HAECs. The nuclei were counterstained with DAPI (blue). Each experiment was performed at least three times. HAECs were transfected with miR-29a-3p or/and miR-29a-3p inhibitor for 48 h and then treated with or without TNFα for 3 h (mRNA detection) or for 6 h (protein detection). A scrambled sequence was used as a negative control (NC). Error bars are defined as the SD. Scale bars, 50 μm. **p < 0.01 indicates statistically significant differences. miR-29a-3p, cells transfected with miR-29a-3p mimic; miR-29a-3p inhibitor, cells transfected with miR-29a-3p inhibitor; miR-29a-3p+inhibitor, cells transfected with miR-29a-3p mimic and its inhibitor.

respectively, suggesting successful transfection (Figure S2). As expected, overexpression of TNF-R1 caused a robust increase in the mRNA levels of VCAM-1 compared to the levels observed in the TNFα group; however, cotransfection with the miR-29a-3p mimic and the TNF-R1-overexpression plasmid partly eliminated this increase. We found that treatment with the miR-29a-3p mimic decreased TNFα-induced mRNA levels of VCAM-1 (Figure 4A), and we observed a similar result here, whereas TNF-R1 overexpres-

sion markedly abrogated the decrease caused by treatment with the miR-29a-3p mimic (Figure 6A). Moreover, the mRNA levels of ICAM-1 and E-selectin presented the same changes (Figures 6B and 6C). Furthermore, the downregulation of TNF-R1 by siRNA effectively negated TNFα-induced VCAM-1, ICAM-1, and E-selectin expression, while cotransfection with the miR-29a-3p inhibitor did not significantly impact their mRNA levels (Figures 6D–6F). The results collectively indicate that miR-29a-3p reduces the
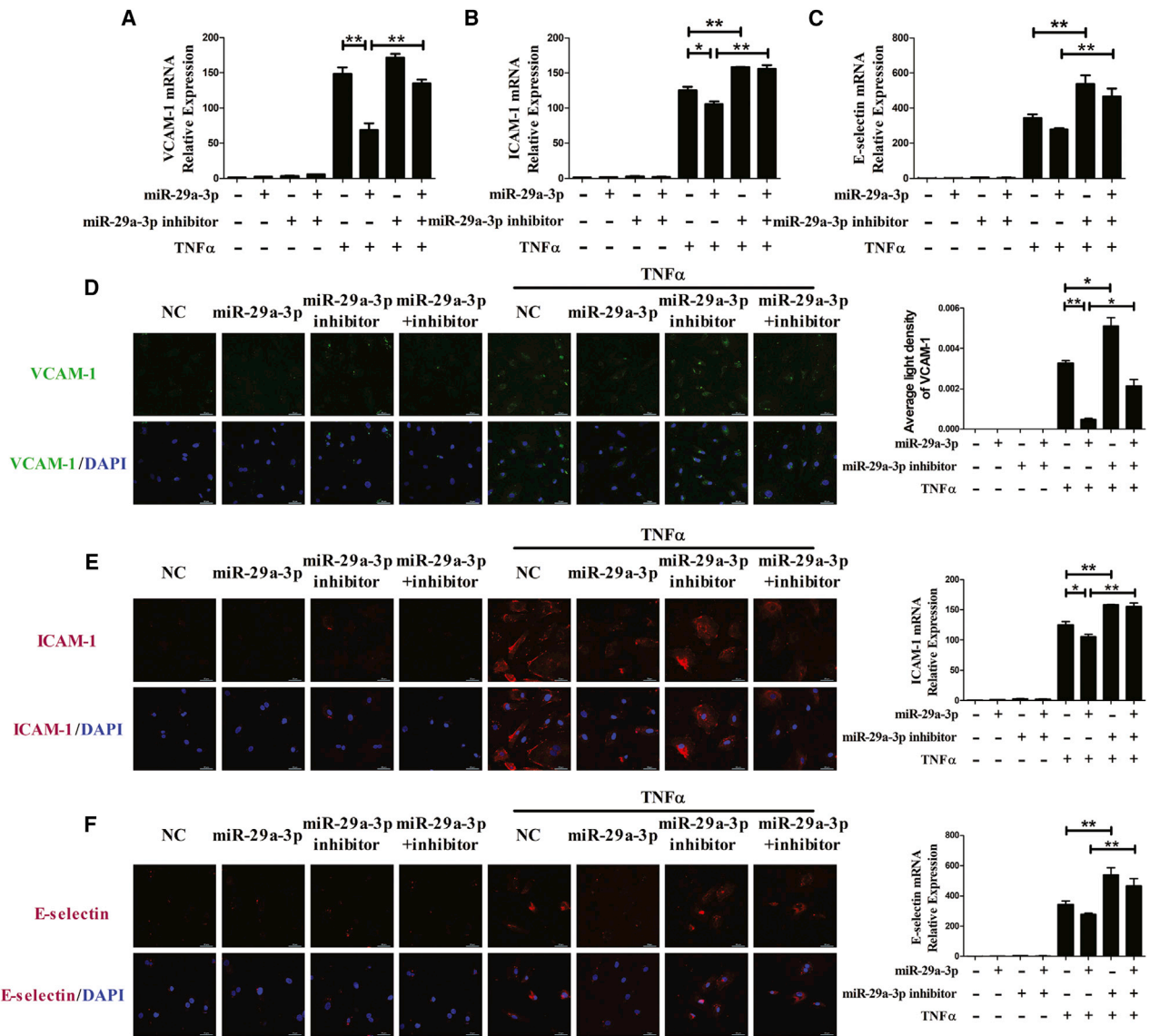
Figure 3. miR-29a-3p Modulates TNFα-Induced VCAM-1, ICAM-1, and E-selectin Expression in pHUVECs

(A–F) The mRNA levels of VCAM-1 (A), ICAM-1 (B), and E-selectin (C) were detected, and the protein expression levels of VCAM-1 (D), ICAM-1 (E), and E-selectin (F) were analyzed by immunofluorescence staining in differentially transfected pHUVECs. The nuclei were counterstained with DAPI (blue). Each experiment was performed at least three times. pHUVECs were transfected with miR-29a-3p or/and miR-29a-3p inhibitor for 48 h and then treated with or without TNFα for 3 h (mRNA detection) or for 6 h (protein detection). A scrambled sequence was used as a negative control (NC). Error bars are defined as the SD. Scale bars, 50 μm. **p < 0.01 indicates statistically significant differences. miR-29a-3p, cells transfected with miR-29a-3p mimic; miR-29a-3p inhibitor, cells transfected with miR-29a-3p inhibitor; miR-29a-3p+inhibitor, cells transfected with miR-29a-3p mimic and its inhibitor.

expression of TNFα-induced adhesion molecules (VCAM-1, ICAM-1, and E-selectin) by targeting TNF-R1.

miR-29a-3p Affects TNF-R1 Expression in the Aortic Endothelium and VCAM-1, ICAM-1, and E-selectin Expression *In Vivo*

To further confirm the results *in vitro*, expression measurements of adhesion molecules (VCAM-1, ICAM-1, and E-selectin) and

TNF-R1 *in vivo* were collected. The mice received a tail vein injection of saline or a miR-29a-3p agomir and an intraperitoneal injection of saline or TNFα (Figure 7A). TNF-R1 expression in frozen sections of aortas was determined by immunohistochemistry staining, and the location of TNF-R1 antigen was indicated by a dark brown diaminobenzidine (DAB) reaction product (Figure 7B). The results indicated that although TNF-R1 expression was decreased in the TNFα group compared with the control
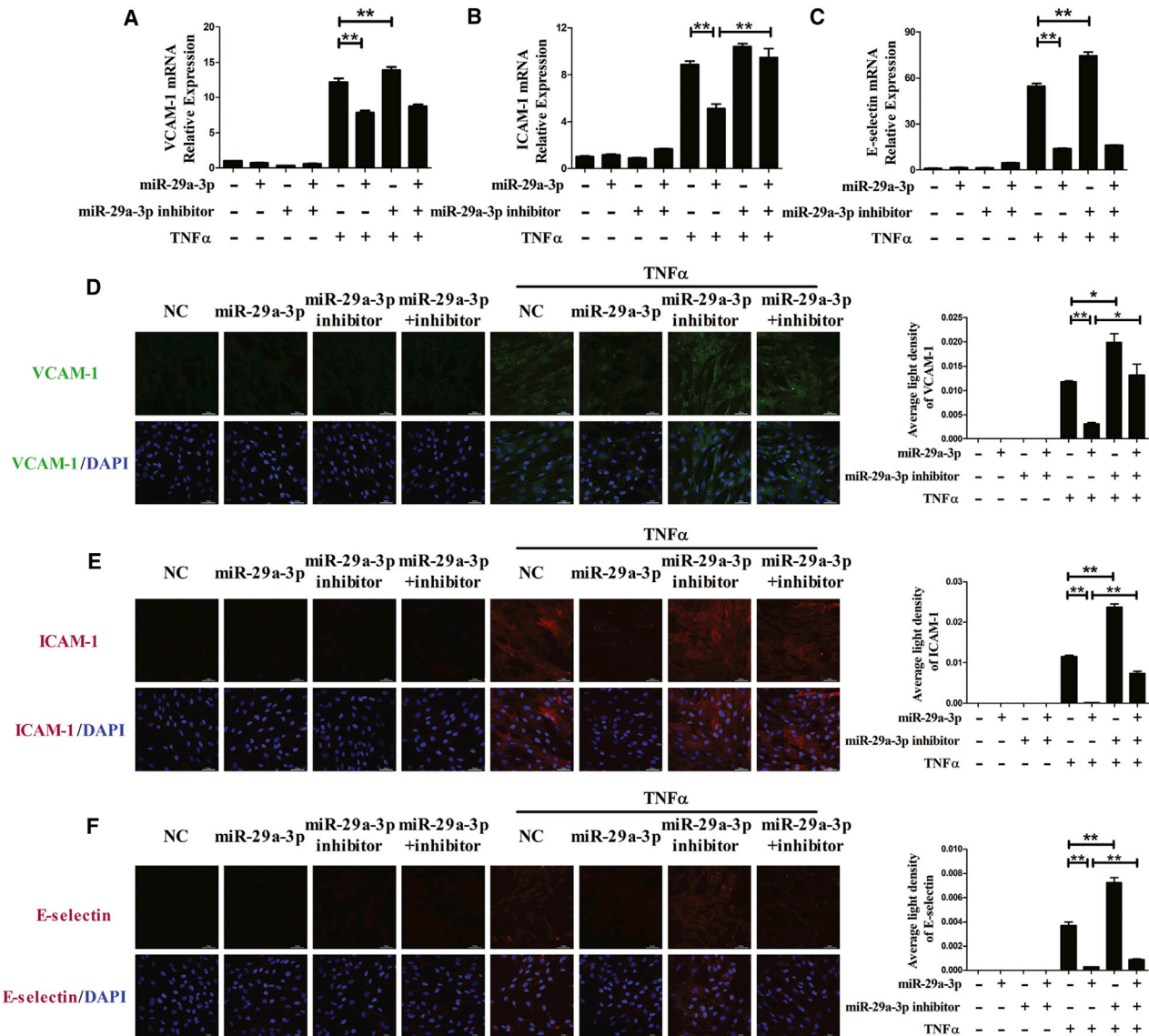
Figure 4. miR-29a-3p Modulates TNFα-Induced VCAM-1, ICAM-1, and E-selectin Expression in HUVSMCs

(A–F) The mRNA levels of VCAM-1 (A), ICAM-1 (B), and E-selectin (C) were detected, and the protein expression levels of VCAM-1 (D), ICAM-1 (E), and E-selectin (F) were analyzed by immunofluorescence staining in differentially transfected HUVSMCs. The nuclei were counterstained with DAPI (blue). Each experiment was performed at least three times. HUVSMCs were transfected with miR-29a-3p or/and miR-29a-3p inhibitor for 48 h and then treated with or without TNFα for 3 h (mRNA detection) or for 6 h (protein detection). A scrambled sequence was used as a negative control (NC). Error bars are defined as the SD. Scale bars, 50 μm. **p < 0.01 indicates statistically significant differences. miR-29a-3p, cells transfected with miR-29a-3p mimic; miR-29a-3p inhibitor, cells transfected with miR-29a-3p inhibitor; miR-29a-3p+inhibitor, cells transfected with miR-29a-3p mimic and its inhibitor.

group, miR-29a-3p overexpression almost entirely eliminated TNF-R1 expression in the aortic endothelium of mice treated with TNFα.

Furthermore, the levels of adhesion molecules in the plasma and in the aortic endothelium were detected by ELISA and immuno-histochemistry staining, respectively. The slides treated with PBS instead of the primary antibody were negative (Figure S3). The results showed that the TNFα treatment increased the levels of VCAM-1, ICAM-1, and E-selectin, and the intervention of miR-29a-3p decreased the elevation of these TNFα-induced adhesion molecules in blood circulation (Figures 8A–8C). Furthermore, similar results were found in the aortic endothelium. TNFα significantly induced the expression, and miR-29a-3p reduced the increases in adhesion molecules mediated by TNFα (Figures 8D–8F).
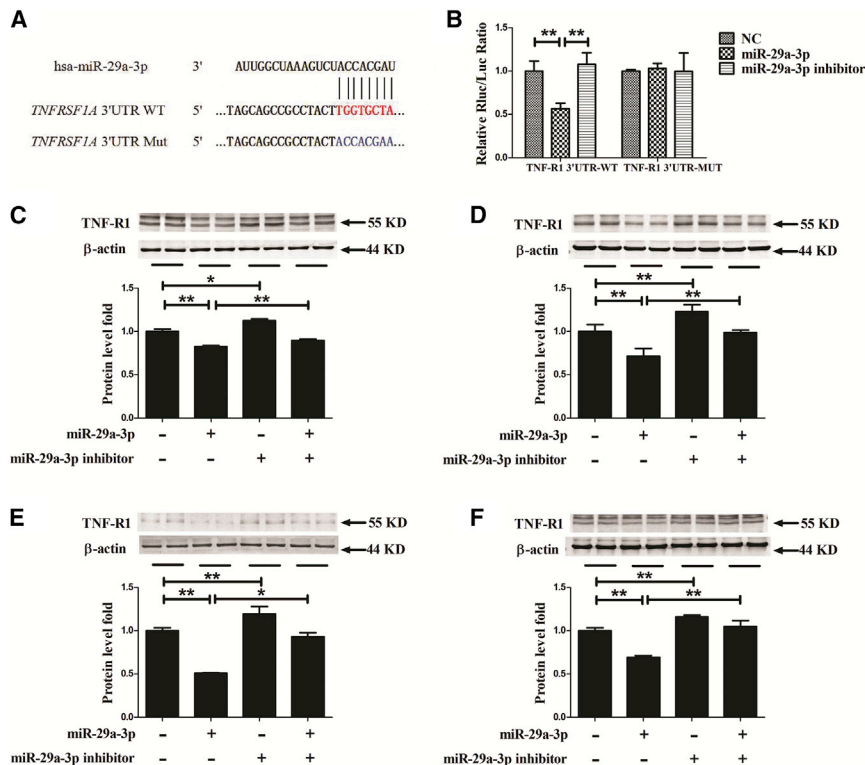
Figure 5. TNF-R1 Expression Is Repressed by miR-29a-3p

(A) Schematic representation of the 3′ UTR of *TNFRSF1A* shows a putative miR-29a-3p binding site. The seed location for the WT 3′ UTR of *TNFRSF1A* is indicated in red, whereas the Mut 3′ UTR is indicated in blue. (B) The effect of miR-29a-3p on the 3′ UTR of *TNFRSF1A* was determined by luciferase activity assays. HEK293 cells were cotransfected with *TNFSF1A*-3′ UTR wild-type (WT) or mutant (Mut) plasmid, and miR-29a-3p or its inhibitor by Lipofectamine 2000. After 24 h, luciferase activities were measured. (C–F) TNF-R1 protein expression was measured in EA.hy926 cells (C), HAECs (D), pHUVECs (E), and HUVSMCs (F) that had been differentially transfected. A scrambled sequence was used as a negative control (NC). After 48 h of transfection, TNF-R1 protein expression was assessed by western blot. Each test was performed at least three times. Error bars are defined as the SD. *p < 0.05 and **p < 0.01 indicate statistically significant differences. miR-29a-3p, cells transfected with miR-29a-3p mimic.

DISCUSSION

In this study, we demonstrated for the first time that miR-29a-3p shows a remarkable inhibitory effect on the expression of TNFα-induced adhesion molecules (VCAM-1, ICAM-1, and E-selectin) in vascular endothelial cells (EA.hy926 cells, HAECs, and pHUVECs) and vascular smooth muscle cells (HUVSMCs); these *in vitro* results were validated with an animal model. The underlying mechanism revealed that TNF-R1, the direct target of miR-29a-3p, mediated the ameliorative role of miR-29a-3p in TNFα-induced endothelial dysfunction.

As a pleiotropic proinflammatory cytokine, TNFα could be used to establish a model of endothelial dysfunction *in vitro* and *in vivo*.[32–35] Likewise, in our experiments, we found that TNFα markedly induced the expression of endothelial dysfunction biomarkers (VCAM-1, ICAM-1, and E-selectin),[36–38] directly providing evidence of the important role of TNFα in endothelial dysfunction.[39–41] In addition, unlike previous reports that used one or two kinds of cells to test their hypotheses, in our study, three kinds of endothelial cells (EA.hy926 cells, pHUVECs, and HAECs) and one kind of vascular smooth muscle cell (HUVSMCs), which also express a variety of cellular adhesion molecules,[42] were used to verify the ameliorative effect of miR-29a-3p on TNFα-induced VCAM-1, ICAM-1, and E-selectin expression. Indeed, elevated levels of adhesion molecules VCAM-1, ICAM-1, and E-selectin, as markers of endothelial dysfunction, play large roles in the progression of atherosclerosis;[11,43–45] thus, the changes in these adhesion molecule levels were measured to assess the degree of endothelial dysfunction in this study. Therefore, the reduction of adhesion molecules caused by the transfection with a miR-29a-3p mimic suggested that miR-29a-3p plays a crucial role in regulating endothelial dysfunction.

Many studies have described the aberrant expression of miR-29 in heart diseases, such as cardiac fibrosis,[20] congestive heart failure,[30] and ischemia-reperfusion injury.[31,46,47] miR-29 has been found to be involved in thoracic aortic development processes,[48] cardiovascular aging,[49] and the pathogenesis of some aortic diseases.[50–53] In particular, Cushing et al.[54] reported that miR-29 was required for postnatal growth and development because of its role in vascular smooth muscle cell differentiation and vessel wall formation; further supporting this role, the authors found a reduction in heart weight in miR-29 null mice. These results imply that miR-29 may play a role in the progression of some cardiovascular diseases. However, little is known regarding the function of miR-29 in the endothelium. Therefore, in this study, we first proposed the protective effects of miR-29 in preventing endothelial dysfunction. This result supports the idea of miR-29 functioning in the modulation of cardiovascular diseases.

TNF-R1 is encoded by *TNFRSF1A* gene and is one of the main TNF receptors; it is responsible for most TNF biological properties, such as antiviral activity and activation of the transcription factor nuclear factor κB (NF-κB), which it does in a wide variety of cell types.[55,56] As is known, the activation of NF-κB is essential for the transcriptional regulation of adhesion molecules VCAM-1, ICAM-1, and E-selectin.[57–60] Furthermore, Zhang et al.[61] reported that inhibition of TNF-R1 controlled aortic atherosclerosis by reducing the expression
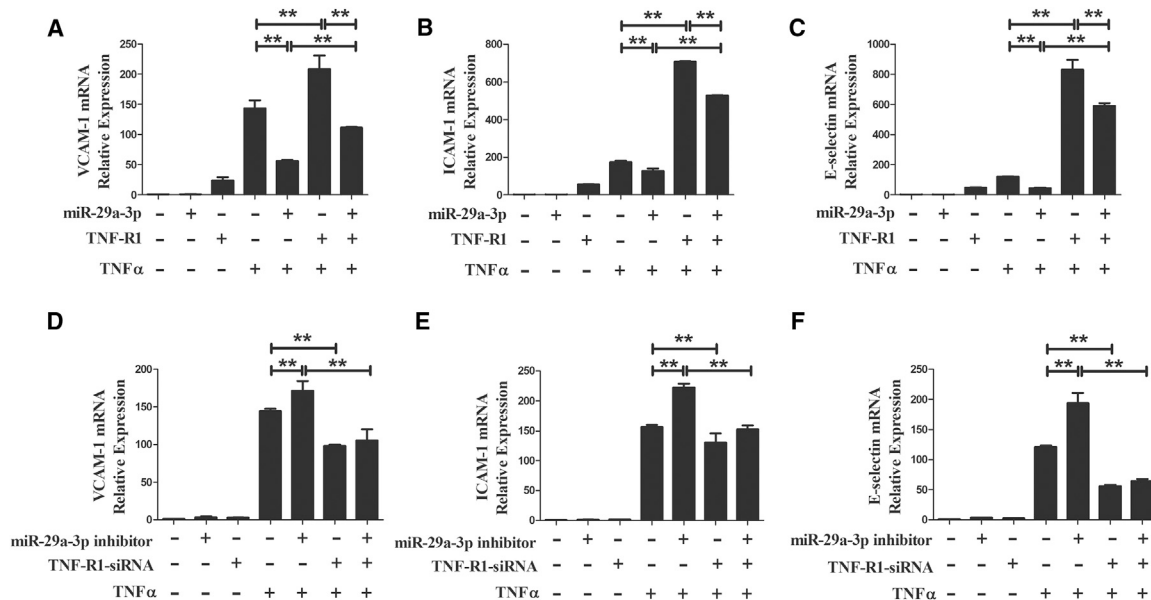
Figure 6. miR-29a-3p Affects TNFα-Induced VCAM-1, ICAM-1, and E-selectin Expression by Targeting TNF-R1

(A–C) The mRNA levels of VCAM-1 (A), ICAM-1 (B), and E-selectin (C) were detected in pHUVECs transfected with miR-29a-3p or/and the plasmid containing human *TNFRSF1A* (TNF-R1 overexpression). (D–F) The mRNA levels of VCAM-1 (D), ICAM-1 (E), and E-selectin (F) were measured in pHUVECs transfected with miR-29a-3p inhibitor or/and TNF-R1-siRNA. After 24 h, the cells were treated with TNFα for 3 h before collection. A scrambled sequence was used as a negative control (NC). Each test was performed three times. Error bars are defined as the SD. *p < 0.05 and **p < 0.01 indicate statistically significant differences. miR-29a-3p, cells transfected with miR-29a-3p mimic.

of the adhesion molecules VCAM-1 and ICAM-1 *in vivo*. In this study, we found that TNF-R1 was a genuine target of miR-29a-3p and verified their relationship for the first time. Therefore, the targeted reduction of TNF-R1 expression by the transfection of the miR-29a-3p mimic might be the reason for the protective effect of miR-29a-3p on TNFα-induced endothelial dysfunction. In this study, the overexpression and inhibition of TNF-R1 were used to confirm this speculation. The data indicate that TNF-R1, as the direct target of miR-29a-3p, mediates the ameliorative role of miR-29a-3p in TNFα-induced endothelial dysfunction.

In conclusion, we have clearly demonstrated that miR-29a-3p remarkably improves TNFα-induced vascular endothelial dysfunction *in vitro* and *in vivo* by targeting TNF-R1. Our findings reveal that regulation of miR-29a-3p may be a potential strategy for the early prevention of atherosclerosis by reducing endothelial dysfunction.

MATERIALS AND METHODS

Reagents

Human TNFα (recombinant human TNFα protein, P01375) and mouse TNFα (recombinant mouse TNFα protein, P06804) were purchased from R&D (Minneapolis, MN, USA). The antibodies used for western blotting were as follows: anti-TNF-R1 (C25C1) was from Cell Signaling Technology (Beverly, MA, USA), and anti-β-actin was from Santa Cruz Biotechnology (Santa Cruz, CA, USA). Antibodies used for immunofluorescence staining were VCAM-1 (551146), ICAM-1 (555511), and E-selectin (551145) (BD Biosciences, Franklin Lakes,

NJ, USA). The antibodies used for immunohistochemistry staining were TNF-R1 (sc-8436, Santa Cruz Biotechnology, Santa Cruz, CA, USA), VCAM-1 (BA0406, Boster Biological Technology, China), ICAM-1 (WL02268, Wanleibio, China), and E-selectin (abs122144a, Absin, China).

Cell Culture, Transfection, and TNFα Treatments

The human endothelial cell line (EA.hy926 cells, ATCC, Manassas, VA, USA), HAECs (BNCC, China), and HEK293 cells (ATCC, Manassas, VA, USA) were maintained in DMEM (HyClone, South Logan, UT, USA) containing 10% fetal bovine serum (FBS; PAA Laboratories, Austria). pHUVECs were obtained from AllCells (China) and cultured incomplete medium (AllCells, China). The HUVSMCs were purchased from ScienCell (Carlsbad, CA, USA) and cultured in basal medium (ScienCell, Carlsbad, CA, USA) with smooth muscle cell growth supplement (ScienCell, Carlsbad, CA, USA) and 10% FBS (PAA Laboratories, Austria). All cells were cultured at 37°C in 5% CO_2 and 95% air atmosphere.

To determine the effects of miR-29a-3p on the expression of the adhesion molecules VCAM-1, ICAM-1, and E-selectin, all cells were transfected with exogenous hsa-miR-29a-3p (miRBase: MIMAT0000086). Specifically, cells were transfected with 50 nM miR-29a-3p mimic (RiboBio, China) or/and 100 nM miR-29a-3p inhibitor (RiboBio, China) with Lipofectamine 2000 reagent (Invitrogen, Carlsbad, CA, USA) according to the manufacturers' protocols. siRNAs against TNF-R1 (TNF-R1-siRNA) were purchased from Santa Cruz
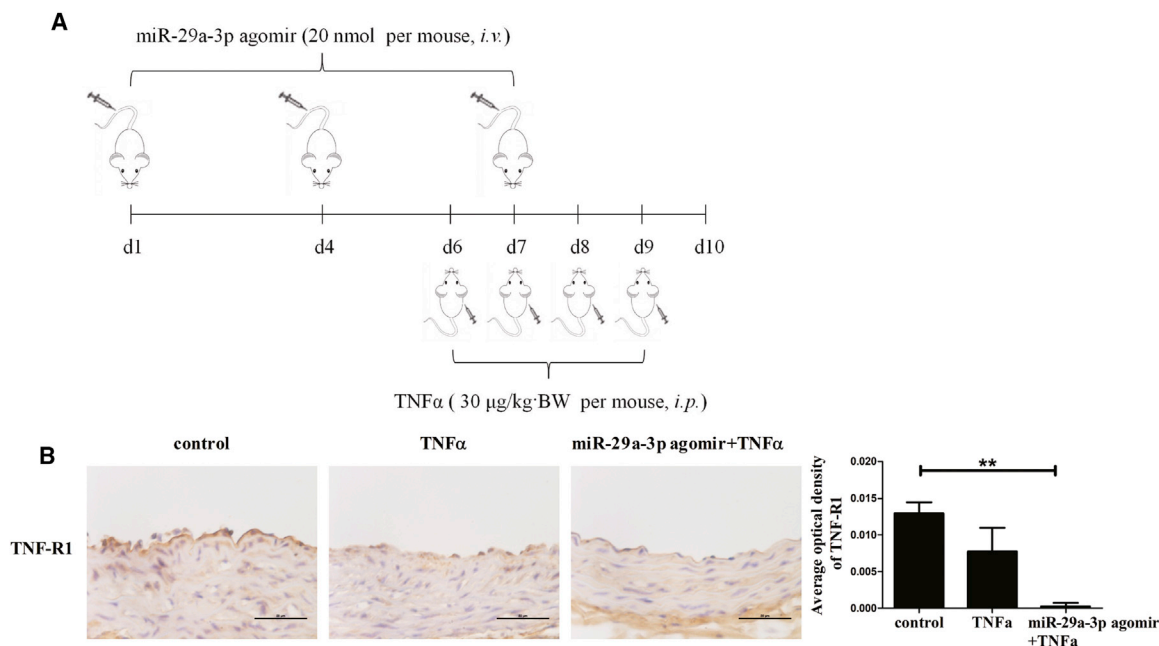
Figure 7. miR-29a-3p Agomir Affects TNF-R1 Expression in Arteries *In Vivo*

(A) Schematic representation of experimental mouse design is shown. Briefly, 8-week-old male mice received a tail vein injection of saline or miR-29a-3p agomir and were then administered an intraperitoneal injection of saline or TNFα. (B) Immunohistochemistry staining was performed for TNF-R1 in the Mouse aorta at harvest. Error bars are defined as the SD. Scale bars, 50 μm. **p < 0.01 indicates statistically significant differences.

Biotechnology (Santa Cruz, CA, USA). The eukaryotic-expressing vector plasmid pDoubleEX-EGFP-*TNFRSF1A* containing the human *TNFRSF1A* (GenBank: NM-001065) gene was constructed by Changsha Yingrun Biotechnology (Yingrun Biotechnology, China) and purified by a Plasmid Midi Kit (QIAGEN, Germany). The pHUVECs were transfected with 100 nM miR-29a-3p inhibitor or/and 100 nM TNF-R1-siRNA. In addition, the pHUVECs were transfected with 50 nM miR-29a-3p mimic or/and the expression vector plasmid pDoubleEX-EGFP-*TNFRSF1A* (TNF-R1 overexpression, 1.5 μg/well). A scrambled sequence was used as a negative control (NC).

Forty-eight hours after the transfection, the cells were treated with or without 10 ng/mL recombinant human TNFα protein (R&D Systems, Minneapolis, MN, USA) for 3 h (to test mRNA levels) or 6 h (to test protein levels), and then they were used for the subsequent experiments. Each *in vitro* test was performed at least three times.

Target Prediction and Luciferase Activity Assay

The target genes of miR-29a-3p were predicted with TargetScan 6.2 (http://www.targetscan.org/). The pmiRRB-REPORTTM Dual-Luciferase reporter vectors carrying the WT or Mut 3′ UTR of *TNFRSF1A* were constructed (RiboBio, China). HEK293 cells were cotransfected with 200 ng of recombinant plasmid, 50 nM miR-29a-3p mimic, or 100 nM miR-29a-3p inhibitor. After 24 h of transfection, the luciferase activities were measured with a Dual-Luciferase reporter assay kit (Promega, Madison, WI, USA) on a luminometer (GloMaxTM 20/20, Promega).

Protein Isolation and Western Blot

Western blotting was performed as previously described[62] with the following primary antibodies: TNF-R1 (Cell Signaling Technology, Danvers, MA, USA) and β-actin (Santa Cruz Biotechnology, Dallas, TX, USA). Anti-rabbit alkaline-phosphatase-conjugated antibody (Promega, Madison, WI, USA) was used as a secondary antibody.

RNA Isolation and Quantitative Real-Time PCR

For mRNA assessment, total RNA was isolated from the treated EA.hy926 cells, HAECs, pHUVECs, and HUVSMCs with different amounts of TRIzol reagent (Invitrogen) according to its manufacturer's instructions. For expression experiments, β-actin was used as an internal control. Primers (VCAM-1, ICAM-1, E-selectin, and β-actin) were synthesized by Invitrogen, and their primer sequences are listed in Table S1. Real-time PCR was performed with a SYBR Green PCR Master Mix by a 7500 Fast Real-Time PCR System (Applied Biosystems, Foster City, CA, USA).[62]

Immunofluorescence Analysis of Cell Surface Expression of VCAM-1, ICAM-1, and E-selectin

Cells were grown to confluence in 24-well plates. After the indicated treatments, the cells were washed with PBS and fixed with 4% paraformaldehyde (PFA). Then the cells were incubated with a fluorescein isothiocyanate (FITC)-conjugated VCAM-1 antibody, a PE-conjugated ICAM-1 antibody, or a PE-conjugated E-selectin antibody (BD Biosciences, Franklin Lakes, NJ, USA) for 48 h. After that, the cell nuclei were counterstained with DAPI (Beyotime Biotechnology,
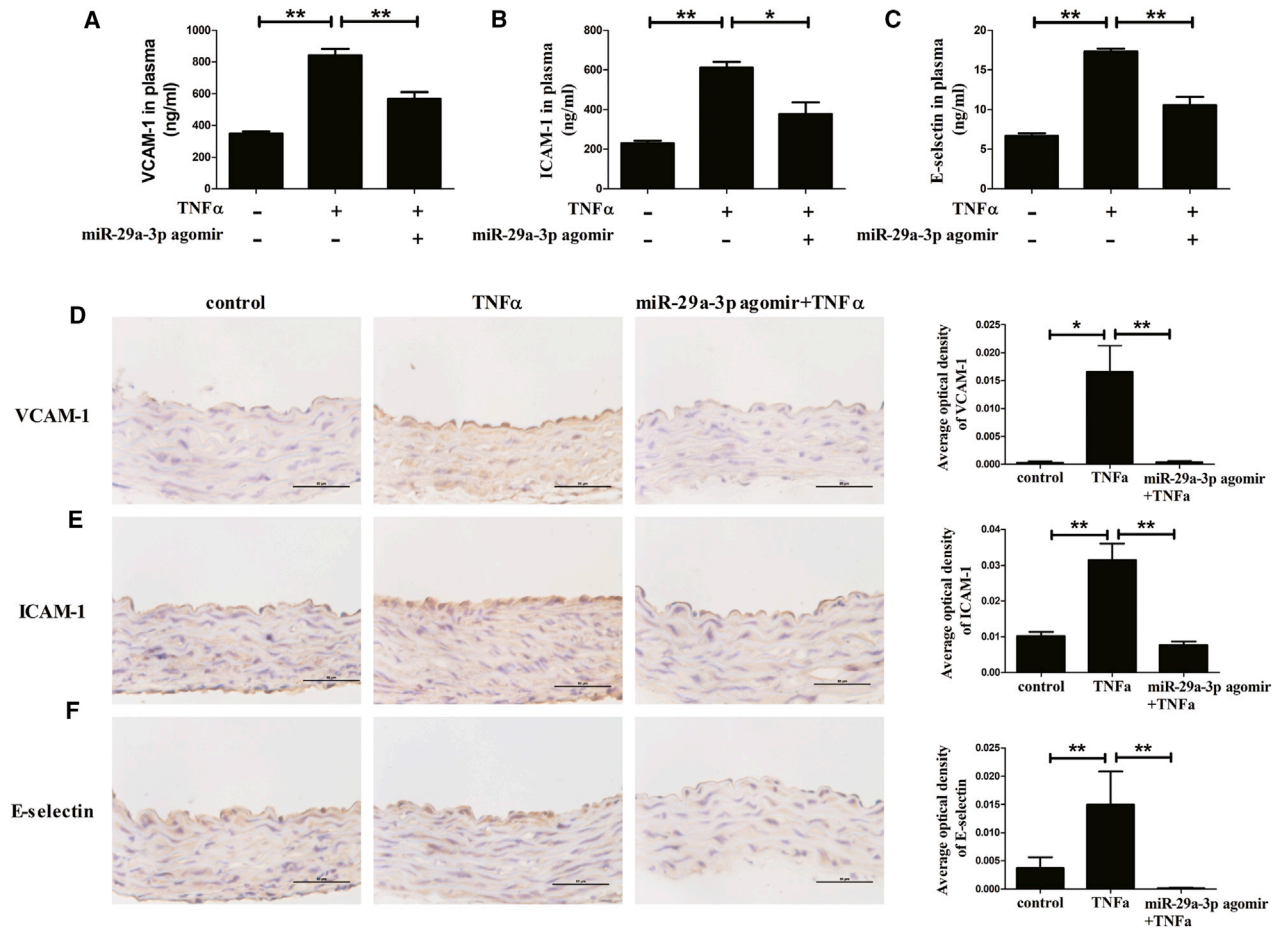
Figure 8. miR-29a-3p Agomir Affects TNFα-Induced VCAM-1, ICAM-1, and E-selectin Expression *In Vivo*

(A–F) The levels of VCAM-1 (A), ICAM-1 (B), and E-selectin (C) in plasma and the expressions of VCAM-1 (D), ICAM-1 (E), and E-selectin (F) in aorta endothelium of mice in different treatment groups were measured by ELISA and immunohistochemistry staining, respectively. The mice received a tail vein injection of saline or miR-29a-3p agomir and were then administered an intraperitoneal injection of saline or TNFα. Error bars are defined as the SD. Scale bars, 50 μm. *p < 0.05 and **p < 0.01 indicate statistically significant differences.

China) for 15 min. The fluorescent signal was detected with a confocal microscope (Nikon, Japan). Image-Pro Plus 6.0 software (Media Cybernetics, Bethesda, MD, USA) was used to calculate the immunofluorescence light intensity. The average light intensity was obtained by summation of light intensity divided by the area of interest.

Animal Experimental Protocol and Adhesion Molecule Analysis

All protocols in this study were approved by the Medical Ethics Committee of Harbin Medical University (China) and were performed in accordance with the NIH regulations for the care and use of animals in research. Twenty C57BL/6 mice (males, 7 weeks old) were used in this experiment (Beijing Vital River Laboratory Animal Technology, China). The mice were maintained on a 12-h light/12-h dark cycle, given water and food *ad libitum*, and housed in an environmentally controlled room at 22 ± 2°C with 50% ± 5% humidity. After an initial acclimation period, the mice were randomly divided into three groups (control, TNFα, and miR-29a-3p agomir + TNFα), with six mice per

group. Based on mmu-miR-29a-3p (miRBase: MIMAT0000535), a miR-29a-3p agomir (micrONTMmmu-miR-29a-3p agomir) was constructed by RiboBio (China). On days 0, 3, and 6, the mice received a tail vein injection (intravenous [i.v.]) of saline or miR-29a-3p agomir (micrONTMmmu-miR-29a-3p agomir, RiboBio, China) at a dose of 20 nmol per mouse, which was administered every 3 days for a total of three injections. On days 6, 7, 8, and 9, the mice were administered an intraperitoneal (i.p.) injection of recombinant mouse TNFα protein (R&D Systems, Minneapolis, MN, USA) at a dose of 30 μg/kg body weight (BW), which they received daily for 3 consecutive days. Saline was used as a negative control over the same period. After the last TNFα injection, all mice were fasted for 12 h and sacrificed under anesthesia with barbital sodium.

Measurements of Adhesion Molecules in Plasma

Mouse plasma was collected by centrifugation of blood in EDTA K2 tubes. Later, the plasma was frozen at −80°C for ELISA analysis.

Plasma VCAM-1, ICAM-1, and E-selectin levels were measured with ELISA kits (Cusabio, China) following the manufacturer's instructions.

Immunohistochemical Localization of TNF-R1, VCAM-1, ICAM-1, and E-selectin

The mouse aorta and heart were perfused with 10 mL of PBS at harvest and dissected from the surrounding tissues. Then, the aortae were submersed in 4% PFA overnight for further measurements. After incubation in PFA, the aortae were washed with PBS and then put in 15% and 30% sucrose in turn until the tissues had successively sunk to the bottom of tubes. Finally, the upper portion of the heart and the proximal aorta were obtained and embedded in an optimal cutting temperature (OCT) compound (Thermo Fisher Scientific, Waltham, MA, USA) and frozen rapidly. The aorta sections were cut at a 6-μm thickness by a cryostat microtome (Thermo Scientific, Cryostar NX70) and stored at −80°C until final analysis.

The presence of TNF-R1, VCAM-1, ICAM-1, and E-selectin in frozen sections was assessed by immunohistochemical staining. The frozen aortic tissue sections were soaked in acetone for fixation, 4% Triton X-100 for permeabilization, and 3% H_2O_2 for removal of endogenous peroxidase, and then they were incubated with blocking reagents (goat serum, Wanleibio, China) overnight to reduce background irritation. Subsequently, the sections were incubated with different primary antibodies for 48 h. Immunohistochemistry for TNF-R1 was performed with a mouse anti-TNF-R1 primary antibody diluted 1:50 (Santa Cruz Biotechnology, CA, USA) and a SABC-POD Mouse IgG kit (Boster Biological Technology, China). To accomplish the immunohistochemistry staining of VCAM-1, ICAM-1, and E-selectin, a rabbit anti-VCAM-1 primary antibody (Boster Biological Technology, China) or a rabbit anti-ICAM-1 primary antibody (Wanleibio, China) or a rabbit anti-E-selectin primary antibody (Absin, China) was used after being diluted with PBS at 1:250, 1:100, and 1:200, respectively. Then, a SABC-POD rabbit IgG kit (Boster Biological Technology, China) was used as a secondary antibody. Next, the signals were visualized by a DAB chromogen system (ZSGB-BIO, China). Cell nuclei were counterstained with Mayer's hematoxylin (Solarbio, China) for 20 min. PBS replaced the primary antibody in negative control slides. Image-Pro Plus 6.0 software was used to calculate the integrated optical intensity. The average optical intensity was obtained by summation of the integrated optical intensity divided by the area of interest.

Statistical Analysis

Values expressed as the mean ± SD were obtained from three separate experiments. The significance of differences was determined by one-way ANOVA. Continuous variables were compared by t tests between two groups. SPSS 10.0 software (SPSS, Chicago, IL, USA) was used for all statistical analyses. $p \leq 0.05$ was considered to indicate a significant difference.

SUPPLEMENTAL INFORMATION

Supplemental Information can be found online at https://doi.org/10.1016/j.omtn.2019.10.014.

AUTHOR CONTRIBUTIONS

Y.L., X.C., and X.D. designed the research. X.D. performed the major parts of the experiments. P.W., X.M., and C.W. performed parts of the research. X.D. analyzed the data, tested statistics, coordinated the figures, and wrote the article. Y.L. and X.C. revised the article.

CONFLICTS OF INTEREST

The authors declare no competing interests.

REFERENCES

1. Ross, R. (1999). Atherosclerosis—an inflammatory disease. N. Engl. J. Med. 340, 115–126.

2. Mizuno, Y., Jacob, R.F., and Mason, R.P. (2011). Inflammation and the development of atherosclerosis. J. Atheroscler. Thromb. 18, 351–358.

3. World Health Organization (2011). In Global Atlas on Cardiovascular Disease Prevention and Control, S. Mendis, P. Puska, and B. Norrving, eds. (World Health Organization), https://apps.who.int/iris/handle/10665/44701.

4. Celermajer, D.S., Sorensen, K.E., Gooch, V.M., Spiegelhalter, D.J., Miller, O.I., Sullivan, I.D., Lloyd, J.K., and Deanfield, J.E. (1992). Non-invasive detection of endothelial dysfunction in children and adults at risk of atherosclerosis. Lancet 340, 1111–1115.

5. Heitzer, T., Schlinzig, T., Krohn, K., Meinertz, T., and Münzel, T. (2001). Endothelial dysfunction, oxidative stress, and risk of cardiovascular events in patients with coronary artery disease. Circulation 104, 2673–2678.

6. Bonetti, P.O., Lerman, L.O., and Lerman, A. (2003). Endothelial dysfunction: a marker of atherosclerotic risk. Arterioscler. Thromb. Vasc. Biol. 23, 168–175.

7. Iantorno, M., and Weiss, R.G. (2014). Using advanced noninvasive imaging techniques to probe the links between regional coronary artery endothelial dysfunction and atherosclerosis. Trends Cardiovasc. Med. 24, 149–156.

8. Horstman, L.L., Jy, W., Jimenez, J.J., and Ahn, Y.S. (2004). Endothelial microparticles as markers of endothelial dysfunction. Front. Biosci. 9, 1118–1135.

9. De Caterina, R., Basta, G., Lazzerini, G., Dell'Omo, G., Petrucci, R., Morale, M., Carmassi, F., and Pedrinelli, R. (1997). Soluble vascular cell adhesion molecule-1 as a biohumoral correlate of atherosclerosis. Arterioscler. Thromb. Vasc. Biol. 17, 2646–2654.

10. Brevetti, G., Martone, V.D., de Cristofaro, T., Corrado, S., Silvestro, A., Di Donato, A.M., Bucur, R., and Scopacasa, F. (2001). High levels of adhesion molecules are associated with impaired endothelium-dependent vasodilation in patients with peripheral arterial disease. Thromb. Haemost. 85, 63–66.

11. Signorelli, S.S., Anzaldi, M., Libra, M., Navolanic, P.M., Malaponte, G., Mangano, K., Quattrocchi, C., Di Marco, R., Fiore, V., and Neri, S. (2016). Plasma levels of inflammatory biomarkers in peripheral arterial disease: results of a cohort study. Angiology 67, 870–874.

12. Bartel, D.P. (2004). MicroRNAs: genomics, biogenesis, mechanism, and function. Cell 116, 281–297.

13. Lee, Y., Kim, M., Han, J., Yeom, K.H., Lee, S., Baek, S.H., and Kim, V.N. (2004). MicroRNA genes are transcribed by RNA polymerase II. EMBO J. 23, 4051–4060.

14. Lim, L.P., Lau, N.C., Garrett-Engele, P., Grimson, A., Schelter, J.M., Castle, J., Bartel, D.P., Linsley, P.S., and Johnson, J.M. (2005). Microarray analysis shows that some microRNAs downregulate large numbers of target mRNAs. Nature 433, 769–773.

15. Pankratz, F., Hohnloser, C., Bemtgen, X., Jaenich, C., Kreuzaler, S., Hoefer, I., Pasterkamp, G., Mastroianni, J., Zeiser, R., Smolka, C., et al. (2018). MicroRNA-

100 suppresses chronic vascular inflammation by stimulation of endothelial auto-phagy. Circ. Res. *122*, 417–432.

16. Suárez, Y., Fernández-Hernando, C., Pober, J.S., and Sessa, W.C. (2007). Dicer dependent microRNAs regulate gene expression and functions in human endothelial cells. Circ. Res. *100*, 1164–1173.

17. Kuehbacher, A., Urbich, C., Zeiher, A.M., and Dimmeler, S. (2007). Role of Dicer and Drosha for endothelial microRNA expression and angiogenesis. Circ. Res. *101*, 59–68.

18. Nazari-Jahantigh, M., Wei, Y., and Schober, A. (2012). The role of microRNAs in arterial remodelling. Thromb. Haemost. *107*, 611–618.

19. Zuo, K., Zhi, K., Zhang, X., Lu, C., Wang, S., Li, M., and He, B. (2015). A dysregulated microRNA-26a/EphA2 axis impairs endothelial progenitor cell function via the p38 MAPK/VEGF pathway. Cell. Physiol. Biochem. *35*, 477–488.

20. van Rooij, E., Sutherland, L.B., Thatcher, J.E., DiMaio, J.M., Naseem, R.H., Marshall, W.S., Hill, J.A., and Olson, E.N. (2008). Dysregulation of microRNAs after myocardial infarction reveals a role of miR-29 in cardiac fibrosis. Proc. Natl. Acad. Sci. USA *105*, 13027–13032.

21. Ulrich, V., Rotllan, N., Araldi, E., Luciano, A., Skroblin, P., Abonnenc, M., Perrotta, P., Yin, X., Bauer, A., Leslie, K.L., et al. (2016). Chronic miR-29 antagonism promotes favorable plaque remodeling in atherosclerotic mice. EMBO Mol. Med. *8*, 643–653.

22. Shen, L., Song, Y., Fu, Y., and Li, P. (2018). miR-29b mimics promotes cell apoptosis of smooth muscle cells via targeting on MMP-2. Cytotechnology *70*, 351–359.

23. Sassi, Y., Avramopoulos, P., Ramanujam, D., Grüter, L., Werfel, S., Giosele, S., Brunner, A.D., Esfandyari, D., Papadopoulou, A.S., De Strooper, B., et al. (2017). Cardiac myocyte miR-29 promotes pathological remodeling of the heart by activating Wnt signaling. Nat. Commun. *8*, 1614.

24. Zhang, Y., Huang, X.R., Wei, L.H., Chung, A.C., Yu, C.M., and Lan, H.Y. (2014). miR-29b as a therapeutic agent for angiotensin II-induced cardiac fibrosis by targeting TGF-β/Smad3 signaling. Mol. Ther. *22*, 974–985.

25. Roderburg, C., Urban, G.W., Bettermann, K., Vucur, M., Zimmermann, H., Schmidt, S., Janssen, J., Koppe, C., Knolle, P., Castoldi, M., et al. (2011). Micro-RNA profiling reveals a role for miR-29 in human and murine liver fibrosis. Hepatology *53*, 209–218.

26. Sekiya, Y., Ogawa, T., Yoshizato, K., Ikeda, K., and Kawada, N. (2011). Suppression of hepatic stellate cell activation by microRNA-29b. Biochem. Biophys. Res. Commun. *412*, 74–79.

27. Qin, W., Chung, A.C., Huang, X.R., Meng, X.M., Hui, D.S., Yu, C.M., Sung, J.J., and Lan, H.Y. (2011). TGF-β/Smad3 signaling promotes renal fibrosis by inhibiting miR-29. J. Am. Soc. Nephrol. *22*, 1462–1474.

28. Pandit, K.V., Milosevic, J., and Kaminski, N. (2011). MicroRNAs in idiopathic pulmonary fibrosis. Transl. Res. *157*, 191–199.

29. Cushing, L., Kuang, P.P., Qian, J., Shao, F., Wu, J., Little, F., Thannickal, V.J., Cardoso, W.V., and Lü, J. (2011). miR-29 is a major regulator of genes associated with pulmonary fibrosis. Am. J. Respir. Cell Mol. Biol. *45*, 287–294.

30. Dawson, K., Wakili, R., Ordog, B., Clauss, S., Chen, Y., Iwasaki, Y., Voigt, N., Qi, X.Y., Sinner, M.F., Dobrev, D., et al. (2013). MicroRNA29: a mechanistic contributor and potential biomarker in atrial fibrillation. Circulation *127*, 1466–1475, 1475e1–28.

31. Ye, Y., Hu, Z., Lin, Y., Zhang, C., and Perez-Polo, J.R. (2010). Downregulation of microRNA-29 by antisense inhibitors and a PPAR-γ agonist protects against myocardial ischaemia-reperfusion injury. Cardiovasc. Res. *87*, 535–544.

32. Keage, H.A., Coussens, S., Kohler, M., Thiessen, M., and Churches, O.F. (2014). Investigating letter recognition in the brain by varying typeface: an event-related potential study. Brain Cogn. *88*, 83–89.

33. Nallasamy, P., Si, H., Babu, P.V., Pan, D., Fu, Y., Brooke, E.A., Shah, H., Zhen, W., Zhu, H., Liu, D., et al. (2014). Sulforaphane reduces vascular inflammation in mice and prevents TNF-α-induced monocyte adhesion to primary endothelial cells through interfering with the NF-κB pathway. J. Nutr. Biochem. *25*, 824–833.

34. Jia, Z., Babu, P.V., Si, H., Nallasamy, P., Zhu, H., Zhen, W., Misra, H.P., Li, Y., and Liu, D. (2013). Genistein inhibits TNF-α-induced endothelial inflammation through the protein kinase pathway A and improves vascular inflammation in C57BL/6 mice. Int. J. Cardiol. *168*, 2637–2645.

35. Li, S., Ning, H., Ye, Y., Wei, W., Guo, R., Song, Q., Liu, L., Liu, Y., Na, L., Niu, Y., et al. (2017). Increasing extracellular Ca^{2+} sensitizes TNF-alpha-induced vascular cell adhesion molecule-1 (VCAM-1) via a TRPC1/ERK1/2/NFκB-dependent pathway

in human vascular endothelial cells. Biochim. Biophys. Acta Mol. Cell Res. *1864*, 1566–1577.

36. O'Brien, K.D., Allen, M.D., McDonald, T.O., Chait, A., Harlan, J.M., Fishbein, D., McCarty, J., Ferguson, M., Hudkins, K., Benjamin, C.D., et al. (1993). Vascular cell adhesion molecule-1 is expressed in human coronary atherosclerotic plaques. Implications for the mode of progression of advanced coronary atherosclerosis. J. Clin. Invest. *92*, 945–951.

37. Zünd, G., Dzus, A.L., McGuirk, D.K., Breuer, C., Shinoka, T., Mayer, J.E., and Colgan, S.P. (1996). Hypoxic stress alone does not modulate endothelial surface expression of bovine E-selectin and intercellular adhesion molecule-1 (ICAM-1). Swiss Surg. Suppl. (*Suppl 1*), 41–45.

38. Nakashima, Y., Raines, E.W., Plump, A.S., Breslow, J.L., and Ross, R. (1998). Upregulation of VCAM-1 and ICAM-1 at atherosclerosis-prone sites on the endothelium in the ApoE-deficient mouse. Arterioscler. Thromb. Vasc. Biol. *18*, 842–851.

39. Ridker, P.M., Hennekens, C.H., Buring, J.E., and Rifai, N. (2000). C-reactive protein and other markers of inflammation in the prediction of cardiovascular disease in women. N. Engl. J. Med. *342*, 836–843.

40. Gerthoffer, W.T. (2007). Mechanisms of vascular smooth muscle cell migration. Circ. Res. *100*, 607–621.

41. Angel, K., Provan, S.A., Fagerhol, M.K., Mowinckel, P., Kvien, T.K., and Atar, D. (2012). Effect of 1-year anti-TNF-α therapy on aortic stiffness, carotid atherosclerosis, and calprotectin in inflammatory arthropathies: a controlled study. Am. J. Hypertens. *25*, 644–650.

42. Wang, X., Feuerstein, G.Z., Gu, J.L., Lysko, P.G., and Yue, T.L. (1995). Interleukin-1β induces expression of adhesion molecules in human vascular smooth muscle cells and enhances adhesion of leukocytes to smooth muscle cells. Atherosclerosis *115*, 89–98.

43. Davies, M.J., Gordon, J.L., Gearing, A.J., Pigott, R., Woolf, N., Katz, D., and Kyriakopoulos, A. (1993). The expression of the adhesion molecules ICAM-1, VCAM-1, PECAM, and E-selectin in human atherosclerosis. J. Pathol. *171*, 223–229.

44. Pearson, T.A., Mensah, G.A., Alexander, R.W., Anderson, J.L., Cannon, R.O., 3rd, Criqui, M., Fadl, Y.Y., Fortmann, S.P., Hong, Y., Myers, G.L., et al.; Centers for Disease Control and Prevention; American Heart Association (2003). Markers of inflammation and cardiovascular disease: application to clinical and public health practice: a statement for healthcare professionals from the Centers for Disease Control and Prevention and the American Heart Association. Circulation *107*, 499–511.

45. Mulvihill, N.T., Foley, J.B., Crean, P., and Walsh, M. (2002). Prediction of cardiovascular risk using soluble cell adhesion molecules. Eur. Heart J. *23*, 1569–1574.

46. Ye, Y., Perez-Polo, J.R., Qian, J., and Birnbaum, Y. (2011). The role of microRNA in modulating myocardial ischemia-reperfusion injury. Physiol. Genomics *43*, 534–542.

47. Zhu, H., and Fan, G.C. (2012). Role of microRNAs in the reperfused myocardium towards post-infarct remodelling. Cardiovasc. Res. *94*, 284–292.

48. Ott, C.E., Grünhagen, J., Jäger, M., Horbelt, D., Schwill, S., Kallenbach, K., Guo, G., Manke, T., Knaus, P., Mundlos, S., and Robinson, P.N. (2011). MicroRNAs differentially expressed in postnatal aortic development downregulate elastin via 3′ UTR and coding-sequence binding sites. PLoS ONE *6*, e16250.

49. Date, K., Ohyama, M., and Ogawa, H. (2015). Carbohydrate-binding activities of coagulation factors fibrinogen and fibrin. Glycoconj. J. *32*, 385–392.

50. Du, Y., Gao, C., Liu, Z., Wang, L., Liu, B., He, F., Zhang, T., Wang, Y., Wang, X., Xu, M., et al. (2012). Upregulation of a disintegrin and metalloproteinase with thrombospondin motifs-7 by miR-29 repression mediates vascular smooth muscle calcification. Arterioscler. Thromb. Vasc. Biol. *32*, 2580–2588.

51. Liao, M., Zou, S., Weng, J., Hou, L., Yang, L., Zhao, Z., Bao, J., and Jing, Z. (2011). A microRNA profile comparison between thoracic aortic dissection and normal thoracic aorta indicates the potential role of microRNAs in contributing to thoracic aortic dissection pathogenesis. J. Vasc. Surg. *53*, 1341–1349.e3.

52. Boon, R.A., Seeger, T., Heydt, S., Fischer, A., Hergenreider, E., Horrevoets, A.J., Vinciguerra, M., Rosenthal, N., Sciacca, S., Pilato, M., et al. (2011). MicroRNA-29 in aortic dilation: implications for aneurysm formation. Circ. Res. *109*, 1115–1119.

53. Maegdefessel, L., Azuma, J., Toh, R., Merk, D.R., Deng, A., Chin, J.T., Raaz, U., Schoelmerich, A.M., Raiesdana, A., Leeper, N.J., et al. (2012). Inhibition of

microRNA-29b reduces murine abdominal aortic aneurysm development. J. Clin. Invest. *122*, 497–506.

54. Cushing, L., Costinean, S., Xu, W., Jiang, Z., Madden, L., Kuang, P., Huang, J., Weisman, A., Hata, A., Croce, C.M., and Lü, J. (2015). Disruption of miR-29 leads to aberrant differentiation of smooth muscle cells selectively associated with distal lung vasculature. PLoS Genet. *11*, e1005238.

55. Puimège, L., Libert, C., and Van Hauwermeiren, F. (2014). Regulation and dysregulation of tumor necrosis factor receptor-1. Cytokine Growth Factor Rev. *25*, 285–300.

56. Wajant, H., Pfizenmaier, K., and Scheurich, P. (2003). Tumor necrosis factor signaling. Cell Death Differ. *10*, 45–65.

57. Chen, J.W., Chen, Y.H., Lin, F.Y., Chen, Y.L., and Lin, S.J. (2003). Ginkgo biloba extract inhibits tumor necrosis factor-α-induced reactive oxygen species generation, transcription factor activation, and cell adhesion molecule expression in human aortic endothelial cells. Arterioscler. Thromb. Vasc. Biol. *23*, 1559–1566.

58. Mukherjee, T.K., Nathan, L., Dinh, H., Reddy, S.T., and Chaudhuri, G. (2003). 17-Epiestriol, an estrogen metabolite, is more potent than estradiol in inhibiting vascular cell adhesion molecule 1 (VCAM-1) mRNA expression. J. Biol. Chem. *278*, 11746–11752.

59. Boyle, E.M., Jr., Kovacich, J.C., Canty, T.G., Jr., Morgan, E.N., Chi, E., Verrier, E.D., and Pohlman, T.H. (1998). Inhibition of nuclear factor-kappa B nuclear localization reduces human E-selectin expression and the systemic inflammatory response. Circulation *98* (19, Suppl), II282–II288.

60. Zhou, Z., Connell, M.C., and MacEwan, D.J. (2007). TNFR1-induced NF-κB, but not ERK, p38MAPK or JNK activation, mediates TNF-induced ICAM-1 and VCAM-1 expression on endothelial cells. Cell. Signal. *19*, 1238–1248.

61. Zhang, L., Peppel, K., Sivashanmugam, P., Orman, E.S., Brian, L., Exum, S.T., and Freedman, N.J. (2007). Expression of tumor necrosis factor receptor-1 in arterial wall cells promotes atherosclerosis. Arterioscler. Thromb. Vasc. Biol. *27*, 1087–1094.

62. Lu, H., Hao, L., Li, S., Lin, S., Lv, L., Chen, Y., Cui, H., Zi, T., Chu, X., Na, L., and Sun, C. (2016). Elevated circulating stearic acid leads to a major lipotoxic effect on mouse pancreatic beta cells in hyperlipidaemia via a miR-34a-5p-mediated PERK/p53-dependent pathway. Diabetologia *59*, 1247–1257.